JOURNAL OF Materials CHEMISTRY

Comparative studies on BN-coatings on SiC and Si_3N_4 nanowires

Chengchun Tang, Yoshio Bando,* Tadao Sato and Keiji Kurashima

Advanced Materials Laboratory and Nanomaterials Laboratory, National Institute for Materials Science, 1-1 Namiki, Tsukuba, Ibaraki 305-0044, Japan

Received 23rd January 2002, Accepted 20th March 2002
First published as an Advance Article on the web 12th April 2002

Uniformly BN-coated silicon carbide nanowires have been synthesized *via* the vapor–liquid–solid growth mechanism. Nanoscale Ni–C grains were used as catalysts and a mixture of boron and silica was heated to simultaneously generate SiO and B_2O_2 vapors. The uniform coating was explained based on the TEM observations. The fixed relative vapor concentrations absorbed by the catalyst droplets and the (111) facets at the outermost surface of the SiC nanowires are responsible for the uniform coating. The effect of the closely packed (111) plane, which exists on the surface of the nanowires, was studied for the tentative synthesis of BN-coated Si_3N_4 nanowires. The BN coating on Si_3N_4 nanowires is disordered due to the lack of a closely packed surface plane. When using a BN supported Ni catalyst, BN nanotubes and nano-bamboos, and crystalline straight or amorphous curved Si_3N_4 nanowires without BN coating are formed.

1. Introduction

Nanoscale one-dimensional structures have sparked great interest in materials research because of their exotic electronic and mechanical properties.[1,2] Aside from carbon and BN nanotubes,[3,4] silicon[5,6] and its carbide (SiC)[7] and nitride (Si_3N_4)[8] nanowires (nanorods) have received widespread interest since they have been expected to possess special properties that may be useful in nanoscale engineering and electronics. Especially considering chemical stability, thermal shock resistance and excellent creep resistance of SiC and Si_3N_4,[9,10] they should be promising materials for the fabrication of electronic devices operating at high temperature, high power, and high frequency, and in harsh environments.[11] The most promising applications for SiC and Si_3N_4 nanowires should be in the field of ceramics and ceramic strengthening, and recent research has also confirmed that the strength and ductility of nanostructured ceramics and nanoscale whiskers are greatly superior to those on the micrometer scale.[12,13]

However, when using these nanowires to strengthen ceramics (especially for oxide ceramics) by incorporating nanowires into the ceramic matrix, the nanowire/matrix interactions have to be considered. In most cases, the interactions will reduce the effects of the nanowires enhancement and consequently the strength of the composites is not significantly improved over the strength of the pure matrix, as observed in the case of SiC whiskers strengthening Al_2O_3 ceramic.[14] Moreover, taking into account their large surface areas, the nanowires should exhibit stronger nanowire/matrix interactions. Therefore, it has been suggested that a feasible strategy might be to use a boron nitride (BN) coating on these nanowires[15–17] due to the chemical inertness of BN at high temperature. In fact, BN coating of nanoscale one-dimensional materials other than SiC and Si_3N_4 nanowires should be valuable for providing the separately insulating layer between the nanoelectronic component and its substrate, or forming the insulating parts in various heterostructural nanodevices, due to the wide band gap of BN of about 5.5 eV, which is independent of the geometric morphology.[18]

SiC nanowires (nanorods) were first synthesized by a carbon nanotube-confined reaction[19] and the nanowire growth mechanism has been attributed as shape memory synthesis in crystallography.[20] The method was also expanded to synthesize BN nanotubes filled with SiC nanowires.[21] Other SiC nanowires with amorphous silica[22,23] or B–N–C wrappers[24] have been synthesized. However, the coatings of the nanowires mentioned above usually vary a great deal in quality and purity and, unfortunately, do not provide uniform coatings over the entire surface of the nanowires. The poorly crystallized and non-uniform coatings adversely affect the thermomechanical and electronic properties of the composites.

Here we report experimental details of a BN coating on the surface of SiC and Si_3N_4 nanowires synthesized by *in-situ* growth of BN and SiC nanowires from nanoscale catalytic droplets. The method is still within the framework of the well-known vapor–liquid–solid mechanism,[25] which has been widely used to synthesize whiskers and was recently developed also for the synthesis of various nanowires, such as Si, Ge, BN, SiC, Al_2O_3, GaN and other one-dimensional nanoscale materials.[5,26–29]

2. Experimental procedure

Two nanoscale catalysts used in this study were prepared by sputtering metallic nickel onto the surfaces of a highly oriented pyrolitic graphite (HOPG–Ni catalyst) sheet and a piece of hexagonal BN (BN–Ni catalyst), respectively. Before sputtering, HOPG and BN were cleaned in acetone several times to remove any absorbed species and then placed into a vacuum chamber. Ni was deposited to a controlled thickness of about 5–10 nm as measured by a quartz crystal monitor. The as-prepared catalyst was then annealed at 500 °C overnight in flowing argon in order to form Ni nanoparticles. A mixture of B and SiO_2 with a molar ratio of 1 : 1 was used as reactants for providing gas precursors for the formation of BN and SiC. About 1 g of the mixture was thoroughly mixed by ball-milling for 6 hours.

A RF induction furnace was used for the nanowire synthesis. The catalyst substrate and the mixture were charged into a BN crucible, which was then placed into a graphite susceptor that was heated from outside by the RF furnace. The location of the catalyst substrate relative to the mixture of B and SiO_2 was adjusted to keep the substrate at 1400 °C when the mixture was heated to 1500 °C. The geometry and vapor transport direction are shown in Fig. 1. The reaction system was held in a flowing protective and transport gas during reaction, and the gas mixed with the reacting gas near the catalyst substrate.

When using the HOPG-supported catalyst, nitrogen was used as the reacting gas and argon and nitrogen were respectively adopted as transport gases in order to study the Si_3N_4

 DOI: 10.1039/b200861k

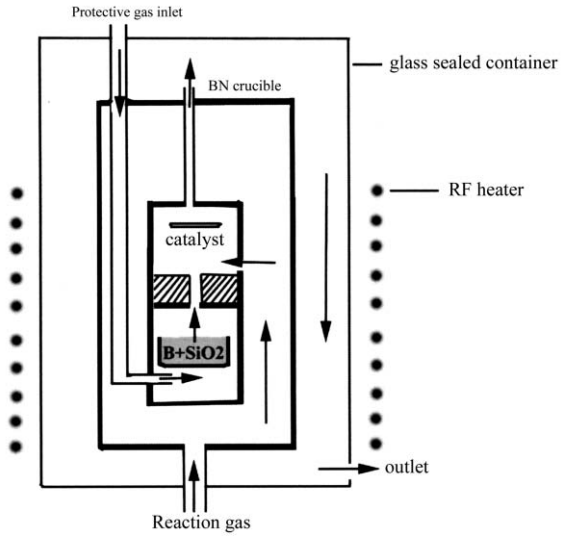

Fig. 1 Schematic of the BN-coated nanowire synthesis apparatus. The arrows indicate the directions of the protecting and reacting gas flows. The reaction chamber was made out of hexagonal BN.

nanowire coating. Ammonia was the reacting gas and argon was the transport gas when using the BN-supported catalyst.

The product was analyzed by X-ray diffraction with Cu Kα radiation (XRD, RINT 2000). The overview of the sample morphology was checked by scanning electron microscopy (SEM). Sample powders were also ultrasonically dispersed in acetone and dropped onto a carbon-coated copper grid for transmission electron microscopy measurements (TEM, JEM-3000F, JEOL) with the analysis systems of energy-dispersive X-ray analysis (EDX) and electron energy loss spectroscopy (EELS).

3. Results and discussions

After reacting for 2 hours, gray products were observed to cover the surface of the catalyst substrate and were physically scraped from the substrate. For the HOPG-supported catalyst, the products were calcined in air to remove the carbon impurity from the catalyst support at 700 °C for 8 hours.

For the HOPG-Ni catalyst, when argon was used as the transport gas and nitrogen as the reacting gas, XRD measurement of the product shows that cubic β-SiC and hexagonal BN (h-BN) are the dominant compositions with a small amount of Si_3N_4 impurity (Fig. 2a). When using nitrogen as the transport gas, the peaks from the Si_3N_4 phase could be apparently observed from the pattern shown in Fig. 2b and β-SiC is still the dominant composition. Due to the very adjacent locations between β-Si_3N_4 (200) and h-BN (002), the pattern from h-BN diffraction could not be observed directly. However, the existence of h-BN could be identified from the broad (200) peak and the h-BN (100) peak. While using the BN–Ni catalyst, nitrogen transport gas and ammonia reacting gas, only Si_3N_4 and h-BN could be observed from the XRD pattern (Fig. 2c).

We speculate that the formation of BN, SiC and Si_3N_4 crystals results from the following chemical reactions:

$$2B\ (s) + 2SiO_2\ (s) \rightarrow B_2O_2\ (g) + 2SiO\ (g) \quad (1)$$

$$B_2O_2\ (g) + 2C\ (s) + N_2\ (g) \rightarrow 2BN\ (s) + 2CO\ (g) \quad (2)$$

$$SiO\ (g) + 2C\ (s) \rightarrow SiC\ (s) + CO\ (g) \quad (3)$$

$$3SiO\ (g) + 3C\ (s) + 2N_2\ (g) \rightarrow Si_3N_4\ (s) + 3CO\ (g) \quad (4)$$

$$B_2O_2\ (g) + 2NH_3\ (g) \rightarrow 2BN\ (s) + 2H_2O\ (g) + H_2\ (g) \quad (5)$$

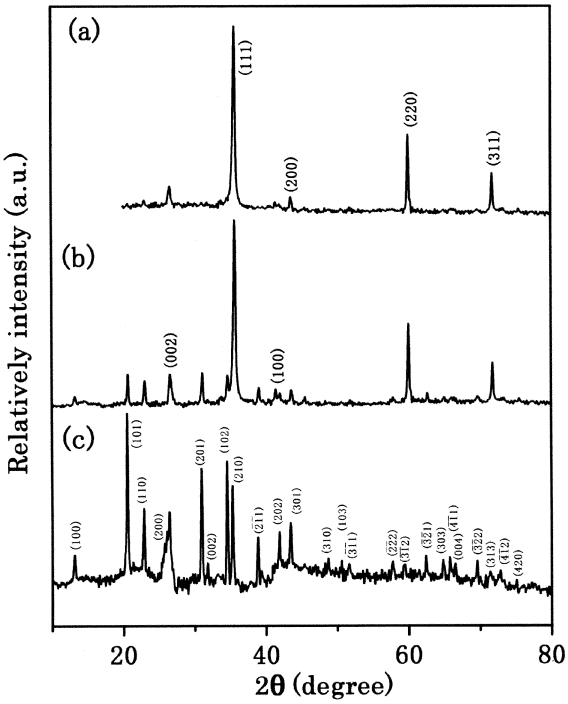

Fig. 2 XRD patterns for the samples synthesized using (a) HOPG–Ni catalyst, argon as transport gas and nitrogen as reacting gas; (b) HOPG–Ni catalyst, nitrogen as transport and reacting gas; (c) BN–Ni catalyst, argon as transport gas and ammonia as reacting gas. The peak positions of SiC, BN and Si_3N_4 are marked by their indices, and shown in (a), (b) and (c), respectively.

$$3SiO\ (g) + 4NH_3\ (g) \rightarrow Si_3N_4\ (s) + 3H_2O\ (g) + 3H_2\ (g) \quad (6)$$

Reaction (1) generates the precursor vapors[30,31] for the formation of BN, SiC and Si_3N_4. It is worth noticing that the concentration of B_2O_2 and SiO has a fixed ratio controlled by reaction (1). For the HOPG–Ni system, reactions (2) and (3) could be used to explain the formation of BN and SiC when argon was the transport gas, and reaction (4) might be responsible for the formation of Si_3N_4, especially in the presence of the high concentration of nitrogen when nitrogen was used as the transport gas. However, for the BN–Ni catalyst, due to the absence of carbon in the reaction area, only BN and Si_3N_4 could be formed by reactions (5) and (6).

SEM observations for the three products indicate that these samples exhibit nanowire structures with diameters ranging from several nanometers to approaching 100 nm, and lengths of several hundred micrometers. Fig. 3 shows a typical SEM image from a sample synthesized by the argon-transport HOPG–Ni catalytic growth. The catalyst particles could be observed frequently to attach to the ends of SiC nanowires.

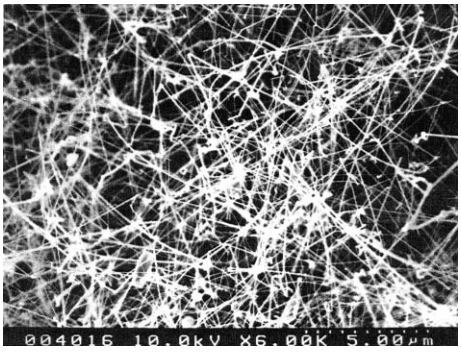

Fig. 3 Typical SEM image of SiC–BN composite nanowires synthesized by argon-transport HOPG–Ni catalytic growth.

EDX analysis shows that the catalysts consist of Ni, Si, B, N and C, and no Ni could be detected in the connected nanowires. Similar results for Si_3N_4 nanowires occurring in the sample from the nitrogen-transport HOPG–Ni catalytic growth could be obtained. These nanowires were grown based on the vapor–liquid–solid growth mechanism. At high temperature, nanoscale Ni particles on the HOPG are in the liquid phase and are incorporated with carbon from HOPG to form Ni–C catalytic droplets. The droplets continuously absorb the reacting vapors of SiO, B_2O_2 and nitrogen and then make the BN and SiC or Si_3N_4 crystal grow when the droplets become saturated. Due to the controlled relative concentrations of SiO and B_2O_2 at the reaction area, the rates of nucleation and growth of the different nanowires are stable.

TEM and high-resolution TEM observations for SiC nanowires, formed by HOPG–Ni catalytic growth under flowing nitrogen or argon gas, indicate that all SiC nanowires are BN composite structures: 2 to 4 nm thick BN layers uniformly coating the overall surface of the SiC nanowires. Fig. 4a shows a typical TEM image of SiC nanowires coated by BN layers. EELS measurement indicates that the coating layers are indeed composed of B and N with a molar ratio of about 1 (Fig. 4b). The BN coating exhibits highly crystallized layers with the distance between two BN layers of 0.34 nm, which is the same as the distance reported in graphitic BN[32] and nanotube BN[4] structures. Most of the SiC nanowires exhibit a high density of stacking faults and microtwins and grow in the [111] axis, as shown in Fig. 4c. The BN layers coat inside the SiC nanowires at the atomic level *via* a slightly distorted BN layer. The selected-area electron diffraction pattern taken from the coating area of the composite nanowire in Fig. 4c is shown in the inset. The different diffraction points from the SiC (1−10) and BN (100) plane could be clearly observed. The BN (002) plane is parallel to the SiC(111) plane. Moreover, for the SiC nanowires with stacking faults and microtwins, there is the corresponding twinned point of BN (002) parallel to the twinned plane of SiC (111). Between BN (002) and its twinned point, many discontinuous diffraction points could be observed, which result from surface transformation due to the stacking faults of the SiC nanowires. All these facts indicate that the BN layer grows on the (111) facet at the outermost surface of the SiC nanowires.

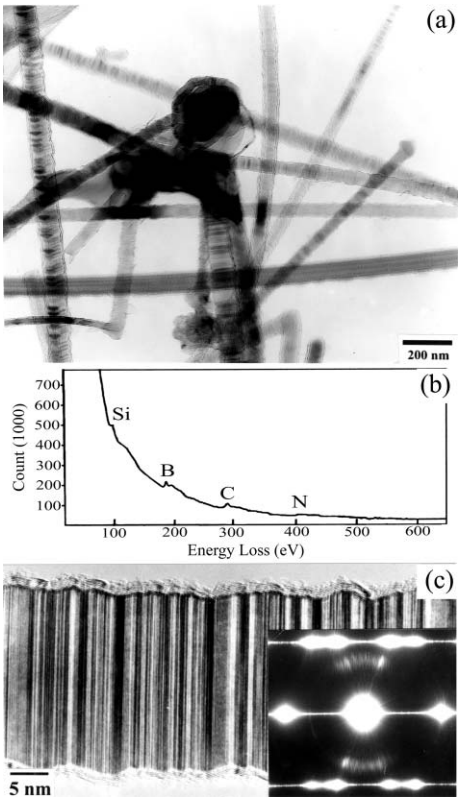

Fig. 4 (a) TEM image of the uniformly BN-coated SiC nanowires; (b) EELS spectrum taken from the coating area; (c) high-resolution TEM image of the BN-coated SiC nanowires, (inset) the selected-area electron diffraction pattern taken the coating area.

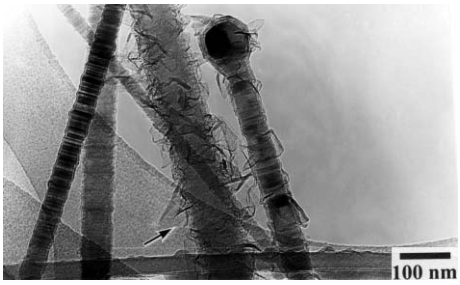

Fig. 5 Typical TEM image for the sample synthesized by nitrogen-transport HOPG–Ni catalytic growth. The arrow points to the disordered BN coated on Si_3N_4 nanowires.

It is difficult to find some Si_3N_4 nanowires from the sample synthesized by HOPG–Ni catalytic growth in the presence of argon as the transport gas, however, the Si_3N_4 nanowires could be found from TEM investigation of the sample with nitrogen as the transport gas. Fig. 5 shows the typical BN-coating morphology. Unlike the coating of SiC nanowires, the BN coatings on the surface of Si_3N_4 nanowires are usually noticeably disordered and do not cover the entire surface of the nanowires.

We believe that the BN-coating mechanism on nanowires is responsible for the failure to coat Si_3N_4 nanowires. As observed for the SiC nanowires, BN basically grows as an epitaxial layer of the closely packed plane, which is (111) for the SiC case. However, for Si_3N_4 nanowires, the next closest packing plane is (100), which is normal to the growth direction of Si_3N_4 nanowires. Due to the lack of plane defects such as stacking faults or microtwins in Si_3N_4 crystals,[33] it therefore is difficult to provide some closely packed facets at the outermost surface of the nanowires for the growth of BN coatings.

When using BN–Ni catalytic growth, one-dimensional BN and Si_3N_4 structures grow separately with different morphologies: Si_3N_4 nanowires grown from the catalysts containing Ni usually exhibit straight rods with diameters of about several tens of nm. Nanotubes and nano-bamboos were found to be the dominant morphologies of the involved BN phase. The Ni catalyst was encapsulated into the bulbous tip of BN nanotubes or into the sealed hollows of BN nano-bamboos. Typical images of the mentioned three morphologies are shown in Fig. 6a. As well as the well-crystallized nanowires and nanotubes, we also frequently observed many amorphous nanowires with diameters uniformly distributed about 20 nm (Fig. 6b). These amorphous nanowires were attached to a nanoparticle at their end. EDX analysis shows the nanoparticle contains Si, N and O, but O could not be detected in the connected nanowires, indicating that they are amorphous SiN_x nanowires. A number of EDX measurements on the attached nanoparticles indicate that no Ni was observed. Therefore, if the VLS mechanism is still responsible for the amorphous nanowires, Si–N–O particles should be the catalysts for the nanowire growth. It is worth noticing that Ni being the VLS catalyst was encapsulated into the inside of the nanowires or nanotubes, and the Si–N–O nanoparticle could also behave as the VLS catalyst. The results imply that the Ni grains have a weak wetting effect on the BN substrate and are easily removed.

The feature of the moveable catalyst also has a strong influence on the BN coating. We occasionally observed cylindrical BN grains attached to the Si_3N_4 nanowires (Fig. 6c). The axial direction of the BN grains is perpendicular to the growth

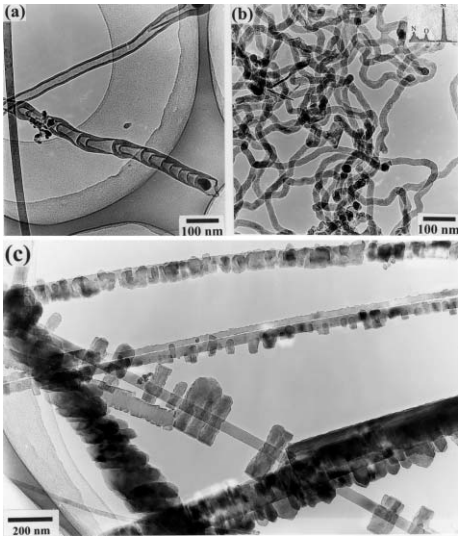

Fig. 6 The morphologies of the sample synthesized using the BN–Ni catalyst: (a) straight Si_3N_4 nanowires without BN coating, and BN nanotubes and nano-bamboo; (b) amorphous SiN_x nanowires, (inset) EDX result from the nanoparticle; (c) BN grains attached to the straight Si_3N_4 nanowires.

direction of the Si_3N_4 nanowires. Obviously, the growth of the BN grains should not be from the catalyst.

4. Conclusion

Uniformly BN-coated SiC nanowires can be synthesized within the framework of the VLS growth mechanism. BN coating layers grow along the (111) facets, which result from the high-density planar defects inside the SiC nanowires. The uniformity of the BN coating is attributed to the existence of the closely packed (111) facets at the outermost surface of the SiC nanowires and the stable BN and SiC growth rates controlled by the formation method of the simultaneously generated B_2O_2 and SiO vapors. Due to the lack of the closely packed facet, a disordered BN coating on Si_3N_4 nanowires is formed when using HOPG-supported catalysts and in the presence of excess nitrogen gas. BN grains were also observed to attach to the Si_3N_4 nanowires synthesized by using the BN-supported catalyst, which more easily results in the formation of BN nanotubes and nano-bamboos, and crystalline or amorphous Si_3N_4 nanowires without the BN coating.

Acknowledgement

One of the authors (C. T.) thanks Y. Gao and F. Xu for great help in transmission electron microscopy characterization.

References

1 X. Duan, Y. Huang, Y. Cui, J. Wang and C. M. Lieber, *Nature*, 2001, **409**, 66.
2 W. A. de Heer, A. Chatelain and D. Ugarte, *Science*, 1995, **270**, 1179.
3 S. Iijima, *Nature*, 1991, **354**, 56.
4 N. C. Chopra, R. J. Luyken, K. Cherry, V. H. Crespi, M. L. Cohen, S. G. Louie and A. Zettl, *Science*, 1995, **269**, 966.
5 A. M. Morales and C. M. Lieber, *Science*, 1998, **279**, 208.
6 Y. F. Zhang, Y. H. Tang, N. Wang, D. P. Yu, C. S. Lee, I. Bello and S. T. Lee, *Appl. Phys. Lett.*, 1998, **72**, 1835.
7 J. Hu, M. Ouyan, P. Yang and C. M. Lieber, *Nature*, 1999, **399**, 48.
8 W. Q. Han, S. S. Fan, Q. Q. Li, B. L. Gu, X. B. Zhang and D. P. Yu, *Appl. Phys. Lett.*, 1997, **71**, 2271.
9 R. Riedel, H. J. Kleebe, H. Schontelder and F. Aldinger, *Nature*, 1995, **374**, 526.
10 G. Ziegler, J. Heinrich and C. Wotting, *J. Mater. Sci.*, 1987, **22**, 3041.
11 A. Fissel, B. Schroter and W. Richter, *Appl. Phys. Lett.*, 1995, **66**, 3182.
12 E. W. Wong, P. E. Sheehan and C. M. Lieber, *Science*, 1997, **277**, 1971.
13 P. Kim and C. M. Lieber, *Science*, 1999, **286**, 2148.
14 K. L. Luthra, *J. Am. Ceram. Soc.*, 1988, **71**, 1114.
15 F. Rebillat, J. Lamon and A. Guette, *Acta Mater.*, 2000, **48**, 4609.
16 S. Sahu, S. Kavecky, L. Illesova, J. Madejova, I. Bertoti and J. Szepvolgyi, *J. Eur. Ceram. Soc.*, 1998, **18**, 1037.
17 R. N. Singh and M. K. Brun, *Adv. Ceram. Mater.*, 1988, **3**, 235.
18 X. Blase, A. Rubio, S. G. Louie and M. L. Cohen, *Eur. Phys. Lett.*, 1994, **28**, 335.
19 H. Dai, E. W. Wong, Y. Z. Lu, S. S. Fan and C. M. Lieber, *Nature*, 1995, **375**, 769.
20 C. Tang, S. Fan, H. Dang, J. Zhao, C. Zhang, P. Li and Q. Gu, *J. Cryst. Growth*, 2000, **210**, 595.
21 W. Han, P. Redlich, F. Ernst and M. Ruhle, *Appl. Phys. Lett.*, 1999, **75**, 1875.
22 L. Zhang, G. Meng and F. Phillipp, *Mater. Sci. Eng. A*, 2000, **286**, 34.
23 Z. L. Wang, Z. R. Dai, R. P. Gao, Z. G. Bai and J. L. Gole, *Appl. Phys. Lett.*, 2000, **77**, 3349.
24 Y. Zhang, K. Suenaga, C. Colliex and S. Iijima, *Science*, 1998, **281**, 973.
25 R. S. Wagner and W. C. Ellis, *Appl. Phys. Lett.*, 1964, **4**, 8.
26 C. Tang, S. Fan, P. Li, M. L. de la Chapelle and H. Dang, *J. Cryst. Growth*, 2001, **224**, 117.
27 S. T. Lee, N. Wang, Y. F. Zhang and Y. H. Tang, *Mater. Res. Bull.*, 1999, 36.
28 C. Tang, S. Fan, H. Dang, P. Li and Y. Liu, *Appl. Phys. Lett.*, 2000, **77**, 1961.
29 D. P. Yu, Z. G. Bai, Y. Ding, Q. L. Huang, H. Z. Zhang, J. J. Wang, Y. H. Zou, W. Qian, G. C. Xiong, H. T. Zhou and S. Q. Feng, *Appl. Phys. Lett.*, 1998, **72**, 3458.
30 J. C. Bailar JR., H. J. Emeleus, R. Nyholm and A. F. Trotman-Dickenson, *Comprehensive Inorganic Chemistry*, Pergamon Press, Oxford, 1964, p. 692.
31 N. A. Toropov and V. P. Barzakovskii, *High-temperature chemistry of silicates and other oxide systems*, Consultants Bureau, New York, 1966, p. 115.
32 R. T. Paine and C. K. Narula, *Chem. Rev.*, 1990, **90**, 73.
33 C. Wang, X. Pan, M. Ruhle, F. L. Riley and M. Mitomo, *J. Mater. Sci.*, 1996, **31**, 5281.